Combining surface effects and non-local two variable refined plate theories on the shear/biaxial buckling and vibration of silver nanoplates

Morteza Karimi, Hojjat Allah Haddad, Ali Reza Shahidi

Department of Mechanical Engineering, Isfahan University of Technology, Isfahan 84156-83111, Iran
E-mail: morteza.karimi@me.iut.ac.ir

Published in Micro & Nano Letters; Received on 2nd December 2014; Accepted on 11th March 2015

In this reported work, surface effects and non-local two variable refined plate theories are combined on the shear/biaxial buckling and vibration of rectangular nanoplates. A silver sheet is selected as the case study to investigate the numerical results. Surface effects are considered by Gurtin-Murdoch's theory. The differential quadrature method is used to solve the governing equations. Differential quadrature solutions are verified by Navier's method. The influences of the non-local parameter on the surface effects of shear/biaxial buckling and vibration are investigated for various boundary conditions. Results show that by increasing the non-local parameter, the effects of surface on the buckling and vibration increase. This result is in contrast with the works of other researchers in the field. Moreover, the non-local effects on the shear buckling and vibration are more important than that of biaxial, whereas the surface effects on the biaxial buckling and vibration are more notable than that of shear.

1. Introduction: Nanoscale structures such as nanoplates and nanobeams have been widely studied by many research groups because of their superior mechanical properties for applications in micro/nanoelectromechanical systems. The main feature of nanostructures is their high surface-to-bulk ratio, which makes the elastic response of their surface layers to be different from macroscale structures. Therefore the classical continuum mechanics cannot describe the surface energy effects. For this reason, some researchers studied surface effects on the bending, buckling and vibration of rectangular nanoplates [1–4] and circular nanoplates [5, 6] based on classical plate theory (CPT). They reported that surface effects could have significant effects on the nanostructures. In addition, increases in the thickness causes reduction of the surface effects. In these works [1–6], the effects of small scale were not taken into account, and because of using classical solutions, for example, Navier's method as used for simply-supported boundary conditions, the above-mentioned researchers were not able to study other boundary conditions. Recently, Ansari *et al.* [7] and Wang and Wang [8] investigated surface effects on the bending, buckling and vibration of nanoplates based on first order shear deformation theory (FSDT) but without considering the non-local effect. They indicated that the significance of surface effects on the response of a nanoplate would rely on its size, type of edge supports and the selected surface constants.

In nanoscale, the non-local effects cannot be ignored. For this reason, some researchers investigated the surface effects on the bending, buckling and vibration of rectangular nanoplates [9], circular nanoplates [10, 11] and nanobeams [12, 13] considering non-local theory. They showed that the deflections and frequencies of nanostructures had a dramatic dependence on the surface effects. In recent years, Mohammadi *et al.* [14, 15] studied the small scale effect on the vibration of nanoplates under biaxial and shear in-plane loads based on CPT. Moreover, Mohammadi *et al.* [16] investigated the shear buckling of orthotropic rectangular nanoplates based on CPT. In these works [14–16], the effects of surface were not considered.

An accurate buckling and vibration analysis of a nanoplate depends closely on the employed plate theory. One of these theories, two variable refined plate theory (TVRPT), was developed by Shimpi [17]. In this regard, Narendar and Gopalakrishnan [18], Narendar [19] and Malekzadeh and Shojaee [20] investigated the buckling and free vibration of rectangular nanoplates based on the non-local elasticity theory. In these works [18–20], surface effects and shear in-plane loads were not investigated. Malekzadeh and Shojaee [21] analysed the influences of non-local and surface effects on the vibration of nanoplates by modifying the original TVRPT. It is interesting to note that they ignored the displacement corresponding to shear, u^s, instead they retained the shear correction factor to the theory. Moreover, Wang and Wang [22, 23] analysed the buckling and vibration of nanoplates combining both surface energy and non-local elasticity theory via FSDT and CPT. They showed [21–23] that by increasing the value of the non-local parameter, the surface effects on the buckling and vibration could decrease. In this Letter, we conclude a reverse result.

We have noted that although some studies have been carried out to analyse surface effects on the buckling and vibrations of nanoplates, with and without including non-local elasticity theory based on the CPT and FSDT, there are no investigations regarding surface effects on the shear/biaxial buckling and vibrations of nanoplates based on TVRPT. In this Letter, surface effects and non-local two variable refined plate theories are combined and investigated regarding the shear/biaxial buckling and vibration of rectangular nanoplates. Small scale and surface effects are considered by the Eringen's non-local and Gurtin-Murdoch's theories, respectively. The differential quadrature method is applied to solve the governing equations for simply-supported and clamped boundary conditions accompanied with their various combinations. For validating the accuracy of the differential quadrature solution, the governing equations are also solved by the classical Navier's method. Moreover, the non-local effects on the surface effects of shear/biaxial buckling and vibration are investigated for various boundary conditions.

2. Formulation: According to Eringen [24], the non-local constitutive behaviour of a Hookean solid can be defined by the following differential constitutive relation

$$(1 - g^2\nabla^2)\sigma_{ij}^{nl} = C_{ijkl}\varepsilon_{kl} \tag{1}$$

where σ_{ij}^{nl}, ε_{kl} and C_{ijkl} are the stress, strain and fourth-order elastic tensor, respectively. ∇^2 is the Laplacian. $g^2 = (e_0a)^2$ is a non-local

doi: 10.1049/mnl.2014.0651

parameter where a is an internal characteristic length and e_0 is a constant. The displacement components in the x, y and z directions consist of bending, b, and shear, s, as follows [18–20]

$$u(x, y, z) = u^{\mathrm{b}} + u^{\mathrm{s}}, \quad v(x, y, z) = v^{\mathrm{b}} + v^{\mathrm{s}}$$
$$w(x, y, z) = w^{\mathrm{b}}(x, y) + w^{\mathrm{s}}(x, y) \tag{2}$$

where

$$u^{\mathrm{b}} = -z\frac{\partial w^{\mathrm{b}}}{\partial x}, \quad v^{\mathrm{b}} = -z\frac{\partial w^{\mathrm{b}}}{\partial y}$$
$$u^{\mathrm{s}} = z\left[\frac{1}{4} - \frac{5}{3}\left(\frac{z}{h}\right)^2\right]\frac{\partial w^{\mathrm{s}}}{\partial x}, \quad v^{\mathrm{s}} = z\left[\frac{1}{4} - \frac{5}{3}\left(\frac{z}{h}\right)^2\right]\frac{\partial w^{\mathrm{s}}}{\partial y} \tag{3}$$

The displacement field can be obtained using (2) and (3) as

$$u(x, y, z) = -z\frac{\partial w^{\mathrm{b}}}{\partial x} + z\left[\frac{1}{4} - \frac{5}{3}\left(\frac{z}{h}\right)^2\right]\frac{\partial w^{\mathrm{s}}}{\partial x}$$
$$v(x, y, z) = -z\frac{\partial w^{\mathrm{b}}}{\partial y} + z\left[\frac{1}{4} - \frac{5}{3}\left(\frac{z}{h}\right)^2\right]\frac{\partial w^{\mathrm{s}}}{\partial y} \tag{4}$$
$$w(x, y, z) = w^{\mathrm{b}}(x, y) + w^{\mathrm{s}}(x, y)$$

It should be noted that unlike the FSDT, this theory does not require a shear correction factor. The linear strain can be obtained from kinematic relations as

$$\begin{Bmatrix} \varepsilon_{xx} \\ \varepsilon_{yy} \\ \gamma_{xy} \end{Bmatrix} = \begin{Bmatrix} \varepsilon^{\mathrm{b}}_{xx} \\ \varepsilon^{\mathrm{b}}_{yy} \\ \gamma^{\mathrm{b}}_{xy} \end{Bmatrix} + \begin{Bmatrix} \varepsilon^{\mathrm{s}}_{xx} \\ \varepsilon^{\mathrm{s}}_{yy} \\ \gamma^{\mathrm{s}}_{xy} \end{Bmatrix}, \quad \begin{Bmatrix} \varepsilon^{\mathrm{b}}_{xx} \\ \varepsilon^{\mathrm{b}}_{yy} \\ \gamma^{\mathrm{b}}_{xy} \end{Bmatrix} = z\begin{Bmatrix} \kappa^{\mathrm{b}}_{xx} \\ \kappa^{\mathrm{b}}_{yy} \\ \kappa^{\mathrm{b}}_{xy} \end{Bmatrix}$$
$$\begin{Bmatrix} \varepsilon^{\mathrm{s}}_{xx} \\ \varepsilon^{\mathrm{s}}_{yy} \\ \gamma^{\mathrm{s}}_{xy} \end{Bmatrix} = f\begin{Bmatrix} \kappa^{\mathrm{s}}_{xx} \\ \kappa^{\mathrm{s}}_{yy} \\ \kappa^{\mathrm{s}}_{xy} \end{Bmatrix}, \quad \begin{Bmatrix} \gamma_{yz} \\ \gamma_{xz} \end{Bmatrix} = \varphi\begin{Bmatrix} \partial w^{\mathrm{s}}/\partial y \\ \partial w^{\mathrm{s}}/\partial x \end{Bmatrix}$$
$$\begin{Bmatrix} \kappa^{\mathrm{b}}_{xx} \\ \kappa^{\mathrm{b}}_{yy} \\ \kappa^{\mathrm{b}}_{xy} \end{Bmatrix} = \begin{Bmatrix} -\partial^2 w^{\mathrm{b}}/\partial x^2 \\ -\partial^2 w^{\mathrm{b}}/\partial y^2 \\ -2\partial^2 w^{\mathrm{b}}/\partial x\partial y \end{Bmatrix}, \quad \begin{Bmatrix} \kappa^{\mathrm{s}}_{xx} \\ \kappa^{\mathrm{s}}_{yy} \\ \kappa^{\mathrm{s}}_{xy} \end{Bmatrix} = \begin{Bmatrix} -\partial^2 w^{\mathrm{s}}/\partial x^2 \\ -\partial^2 w^{\mathrm{s}}/\partial y^2 \\ -2\partial^2 w^{\mathrm{s}}/\partial x\partial y \end{Bmatrix}$$
$$f = -\frac{1}{4}z + \frac{5}{3}z\left(\frac{z}{h}\right)^2, \quad \varphi = \frac{5}{4} - 5\left(\frac{z}{h}\right)^2 \tag{5}$$

For an isotropic nanoplate, the stress–strain relation of a bulk material are expressed by

$$\begin{Bmatrix} \sigma^{\mathrm{b}}_{xx} \\ \sigma^{\mathrm{b}}_{yy} \\ \sigma^{\mathrm{b}}_{xy} \end{Bmatrix} = \begin{bmatrix} C_{11} & C_{12} & 0 \\ C_{21} & C_{22} & 0 \\ 0 & 0 & C_{66} \end{bmatrix}\begin{Bmatrix} \varepsilon^{\mathrm{b}}_{xx} \\ \varepsilon^{\mathrm{b}}_{yy} \\ \gamma^{\mathrm{b}}_{xy} \end{Bmatrix}$$
$$\begin{Bmatrix} \sigma^{\mathrm{s}}_{xx} \\ \sigma^{\mathrm{s}}_{yy} \\ \sigma^{\mathrm{s}}_{xy} \end{Bmatrix} = \begin{bmatrix} C_{11} & C_{12} & 0 \\ C_{21} & C_{22} & 0 \\ 0 & 0 & C_{66} \end{bmatrix}\begin{Bmatrix} \varepsilon^{\mathrm{s}}_{xx} \\ \varepsilon^{\mathrm{s}}_{yy} \\ \gamma^{\mathrm{s}}_{xy} \end{Bmatrix} \tag{6}$$
$$\begin{Bmatrix} \sigma_{yz} \\ \sigma_{xz} \end{Bmatrix} = \begin{bmatrix} C_{44} & 0 \\ 0 & C_{55} \end{bmatrix}\begin{Bmatrix} \gamma_{yz} \\ \gamma_{xz} \end{Bmatrix}$$

where the elastic constants C_{ij} are in terms of the Young's modulus, E, and Poisson's ratio, v

$$C_{11} = C_{22} = \frac{E}{1 - \nu^2}, \quad C_{12} = C_{21} = \frac{\nu E}{1 - \nu^2}$$
$$C_{44} = C_{55} = C_{66} = G \tag{7}$$

where G is the shear modulus. The constitutive relations of the surface layers s^+ and s^-, as given by Gurtin and Murdoch [25], can be defined as

$$\sigma^{\mathrm{s}\pm}_{\alpha\beta} = \tau^{\mathrm{s}\pm}(\delta_{\alpha\beta} + u_{\alpha,\beta}) + (\mu^{\mathrm{s}\pm} - \tau^{\mathrm{s}\pm})(u_{\alpha,\beta} + u_{\beta,\alpha})$$
$$+ (\lambda^{\mathrm{s}\pm} + \tau^{\mathrm{s}\pm})u_{\gamma,\gamma}\delta_{\alpha\beta}, \quad \alpha, \beta, \gamma = x, y \quad \left(z = \pm\frac{h}{2}\right)$$
$$\sigma^{\mathrm{s}\pm}_{\alpha z} = \tau^{\mathrm{s}\pm}u_{z,\alpha}, \quad \alpha = x, y \tag{8}$$

where $\delta_{\alpha\beta}$ is the Kronecker delta and $\alpha = \beta = \gamma = x, y$. $\tau^{\mathrm{s}\pm}$, $\lambda^{\mathrm{s}\pm}$ and $\mu^{\mathrm{s}\pm}$ are the residual surface tension under unconstrained conditions, and the surface Lame constants on the s^+ and s^- surfaces, respectively. If the top and bottom layers have the same material properties, the stress–strain relations become

$$\begin{Bmatrix} \sigma^{\mathrm{b,s}\pm}_{xx} \\ \sigma^{\mathrm{b,s}\pm}_{yy} \\ \sigma^{\mathrm{b,s}\pm}_{xy} \end{Bmatrix} = \pm\frac{h}{2}\begin{bmatrix} (2\mu^{\mathrm{s}} + \lambda^{\mathrm{s}}) & (\tau^{\mathrm{s}} + \lambda^{\mathrm{s}}) & 0 \\ (\tau^{\mathrm{s}} + \lambda^{\mathrm{s}}) & (2\mu^{\mathrm{s}} + \lambda^{\mathrm{s}}) & 0 \\ 0 & 0 & \frac{1}{2}(2\mu^{\mathrm{s}} - \tau^{\mathrm{s}}) \end{bmatrix}$$
$$\times \begin{Bmatrix} \kappa^{\mathrm{b}}_{xx} \\ \kappa^{\mathrm{b}}_{yy} \\ \kappa^{\mathrm{b}}_{xy} \end{Bmatrix} + \begin{bmatrix} \tau^{\mathrm{s}} \\ \tau^{\mathrm{s}} \\ 0 \end{bmatrix}$$
$$\begin{Bmatrix} \sigma^{\mathrm{s,s}\pm}_{xx} \\ \sigma^{\mathrm{s,s}\pm}_{yy} \\ \sigma^{\mathrm{s,s}\pm}_{xy} \end{Bmatrix} = \pm\frac{h}{12}\begin{bmatrix} (2\mu^{\mathrm{s}} + \lambda^{\mathrm{s}}) & (\tau^{\mathrm{s}} + \lambda^{\mathrm{s}}) & 0 \\ (\tau^{\mathrm{s}} + \lambda^{\mathrm{s}}) & (2\mu^{\mathrm{s}} + \lambda^{\mathrm{s}}) & 0 \\ 0 & 0 & \frac{1}{2}(2\mu^{\mathrm{s}} - \tau^{\mathrm{s}}) \end{bmatrix}$$
$$\times \begin{Bmatrix} \kappa^{\mathrm{s}}_{xx} \\ \kappa^{\mathrm{s}}_{yy} \\ \kappa^{\mathrm{s}}_{xy} \end{Bmatrix} + \begin{bmatrix} \tau^{\mathrm{s}} \\ \tau^{\mathrm{s}} \\ 0 \end{bmatrix}$$
$$\begin{Bmatrix} \sigma^{\mathrm{s}\pm}_{yz} \\ \sigma^{\mathrm{s}\pm}_{xz} \end{Bmatrix} = \begin{bmatrix} \tau^{\mathrm{s}} & 0 \\ 0 & \tau^{\mathrm{s}} \end{bmatrix}\begin{Bmatrix} \partial w^{\mathrm{s}}/\partial y \\ \partial w^{\mathrm{s}}/\partial x \end{Bmatrix} \tag{9}$$

The resultant stresses are defined as

$$M^{\mathrm{b}}_{\alpha\beta} = \int_{-h/2}^{h/2} z\sigma^{\mathrm{b}}_{\alpha\beta}\,\mathrm{d}z + (\sigma^{\mathrm{b,s+}}_{\alpha\beta} - \sigma^{\mathrm{b,s-}}_{\alpha\beta})\frac{h}{2} \quad \alpha, \beta = x, y$$
$$M^{\mathrm{s}}_{\alpha\beta} = \int_{-h/2}^{h/2} f\sigma^{\mathrm{s}}_{\alpha\beta}\,\mathrm{d}z + (\sigma^{\mathrm{s,s+}}_{\alpha\beta} - \sigma^{\mathrm{s,s-}}_{\alpha\beta})\frac{h}{2} \quad \alpha, \beta = x, y \tag{10}$$
$$Q_{\alpha z} = \int_{-h/2}^{h/2} \sigma_{\alpha z}\,\mathrm{d}z + (\sigma^{\mathrm{s+}}_{\alpha z} + \sigma^{\mathrm{s-}}_{\alpha z}) \quad \alpha = x, y$$

where $M_{\alpha\beta}$ and $Q_{\alpha\beta}$ are the bending moment and transverse shear force, respectively. Using (1), (4)–(10), the stress resultant can be expressed in terms of the displacement components as (see (11)) where A_{ij} and D_{ij} are called extensional and bending stiffness, respectively

$$D_{11} = D_{22} = D = \frac{Eh^3}{12(1-\nu^2)}, \quad D_{12} = D_{21} = \nu D = \frac{\nu E h^3}{12(1-\nu^2)}$$
$$A_{44} = A_{55} = \frac{5}{6}Gh, \quad D_{66} = \frac{Gh^3}{12} \tag{12}$$

Using Hamilton's principle, the equations of motion, considering both the non-local and surface effects, can be written as [18–21]

$$\begin{aligned}
\delta w^{\mathrm{b}}:& \frac{\partial^2 M_{xx}^{\mathrm{b}}}{\partial x^2} + 2\frac{\partial^2 M_{xy}^{\mathrm{b}}}{\partial x \partial y} + \frac{\partial^2 M_{yy}^{\mathrm{b}}}{\partial y^2} + 2\tau^s \nabla^2(w^{\mathrm{b}} + w^{\mathrm{s}}) + q \\
&+ N_{xx}\frac{\partial^2 (w^{\mathrm{b}} + w^{\mathrm{s}})}{\partial x^2} + 2N_{xy}\frac{\partial^2 (w^{\mathrm{b}} + w^{\mathrm{s}})}{\partial x \partial y} + N_{yy}\frac{\partial^2 (w^{\mathrm{b}} + w^{\mathrm{s}})}{\partial y^2} \\
&= m_0\left(\frac{\partial^2 w^{\mathrm{b}}}{\partial t^2} + \frac{\partial^2 w^{\mathrm{s}}}{\partial t^2}\right) - m_2\left(\frac{\partial^4 w^{\mathrm{b}}}{\partial t^2 \partial x^2} + \frac{\partial^4 w^{\mathrm{b}}}{\partial t^2 \partial y^2}\right) \\
\delta w^{\mathrm{s}}:& \frac{\partial^2 M_{xx}^{\mathrm{s}}}{\partial x^2} + 2\frac{\partial^2 M_{xy}^{\mathrm{s}}}{\partial x \partial y} + \frac{\partial^2 M_{yy}^{\mathrm{s}}}{\partial y^2} + 2\tau^s \nabla^2(w^{\mathrm{b}} + w^{\mathrm{s}}) + q \\
&+ \frac{\partial Q_{xz}}{\partial x} + \frac{\partial Q_{yz}}{\partial y} + N_{xx}\frac{\partial^2 (w^{\mathrm{b}} + w^{\mathrm{s}})}{\partial x^2} \\
&+ 2N_{xy}\frac{\partial^2 (w^{\mathrm{b}} + w^{\mathrm{s}})}{\partial x \partial y} + N_{yy}\frac{\partial^2 (w^{\mathrm{b}} + w^{\mathrm{s}})}{\partial y^2} \\
&= m_0\left(\frac{\partial^2 w^{\mathrm{b}}}{\partial t^2} + \frac{\partial^2 w^{\mathrm{s}}}{\partial t^2}\right) - \frac{m_2}{84}\left(\frac{\partial^4 w^{\mathrm{s}}}{\partial t^2 \partial x^2} + \frac{\partial^4 w^{\mathrm{s}}}{\partial t^2 \partial y^2}\right)
\end{aligned} \tag{13}$$

where N_{xx}, N_{yy}, N_{xy} and q are the in-plane and out-of-plane applied loads, respectively. m_0 and m_2 are the mass inertias defined as

$$(m_0, m_2) = \int_{-h/2}^{h/2} \rho(1, z^2)\,\mathrm{d}z \tag{14}$$

The vibration response is harmonic; therefore the deflection because of vibrations of a thin plate can be expressed as

$$\begin{aligned}
w^{\mathrm{b}}(x, y, t) &= W^{\mathrm{b}}(x, y)\mathrm{e}^{i\omega t} \\
w^{\mathrm{s}}(x, y, t) &= W^{\mathrm{s}}(x, y)\mathrm{e}^{i\omega t}
\end{aligned} \tag{15}$$

where ω is the natural frequency and $i^2 = -1$. Using (11)–(15) and assuming $q = 0$, the equations of motion for rectangular nanoplates

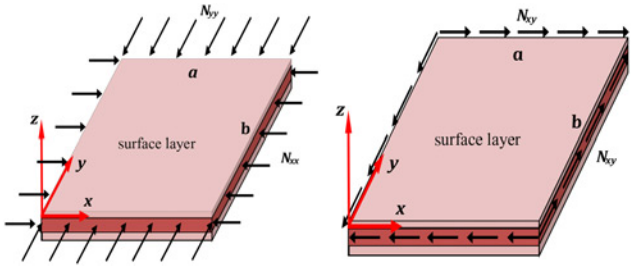

Figure 1 *Geometry of rectangular nanoplate with surface layers showing biaxial loading (a) and shear loading (b)*

can be expressed in terms of displacements W^{b} and W^{s}, as follows

$$\begin{aligned}
&\left(D + \frac{E^s h^2}{2}\right)(\nabla^4 W^{\mathrm{b}}) - 2\tau^s\{(1 - g^2\nabla^2)\nabla^2(W^{\mathrm{b}} + W^{\mathrm{s}})\} \\
&\quad - (1 - g^2\nabla^2)\left\{N_{xx}\left(\frac{\partial^2 W^{\mathrm{b}}}{\partial x^2} + \frac{\partial^2 W^{\mathrm{s}}}{\partial x^2}\right)\right. \\
&\quad \left. + 2N_{xy}\left(\frac{\partial^2 W^{\mathrm{b}}}{\partial xy} + \frac{\partial^2 W^{\mathrm{s}}}{\partial xy}\right) + N_{yy}\left(\frac{\partial^2 W^{\mathrm{b}}}{\partial y^2} + \frac{\partial^2 W^{\mathrm{s}}}{\partial y^2}\right)\right\} \\
&\quad - \omega^2\{(1 - g^2\nabla^2)\left(m_0(W^{\mathrm{b}} + W^{\mathrm{s}}) - m_2\nabla^2(W^{\mathrm{b}})\right)\} = 0 \\
&\frac{1}{84}\left\{\left(D + \frac{E^s h^2}{12}\right)(\nabla^4 W^{\mathrm{s}})\right\} - 2\tau^s\{(1 - g^2\nabla^2)\nabla^2(W^{\mathrm{b}} + W^{\mathrm{s}})\} \\
&\quad - (A_{55} + 2\tau^s)\frac{\partial^2 W^{\mathrm{s}}}{\partial x^2} - (A_{44} + 2\tau^s)\frac{\partial^2 W^{\mathrm{s}}}{\partial y^2} \\
&\quad - (1 - g^2\nabla^2)\left\{N_{xx}\left(\frac{\partial^2 W^{\mathrm{b}}}{\partial x^2} + \frac{\partial^2 W^{\mathrm{s}}}{\partial x^2}\right)\right. \\
&\left. + 2N_{xy}\left(\frac{\partial^2 W^{\mathrm{b}}}{\partial xy} + \frac{\partial^2 W^{\mathrm{s}}}{\partial xy}\right) + N_{yy}\left(\frac{\partial^2 W^{\mathrm{b}}}{\partial y^2} + \frac{\partial^2 W^{\mathrm{s}}}{\partial y^2}\right)\right\} \\
&\quad - \omega^2\left\{(1 - g^2\nabla^2)\left(m_0(W^{\mathrm{b}} + W^{\mathrm{s}}) - \frac{m_2}{84}\nabla^2(W^{\mathrm{s}})\right)\right\} = 0
\end{aligned} \tag{16}$$

where $E^s = 2\mu^s + \lambda^s$. Fig. 1 shows the geometry of the rectangular nanoplate and the loading conditions.

3. Solution procedure

3.1. Navier's method: Based on Navier's method, the exact solutions for biaxial buckling and vibration, regarding the

$$\begin{aligned}
(1 - g^2\nabla^2)\begin{Bmatrix} M_{xx}^{\mathrm{b}} \\ M_{yy}^{\mathrm{b}} \\ M_{xy}^{\mathrm{b}} \end{Bmatrix} &= \left\{\begin{bmatrix} D_{11} & D_{12} & 0 \\ D_{12} & D_{22} & 0 \\ 0 & 0 & D_{66} \end{bmatrix} + \frac{h^2}{2}\begin{bmatrix} (2\mu^s + \lambda^s) & (\tau^s + \lambda^s) & 0 \\ (\tau^s + \lambda^s) & (2\mu^s + \lambda^s) & 0 \\ 0 & 0 & \frac{1}{2}(2\mu^s - \tau^s) \end{bmatrix}\right\}\begin{Bmatrix} \kappa_{xx}^{\mathrm{b}} \\ \kappa_{yy}^{\mathrm{b}} \\ \kappa_{xy}^{\mathrm{b}} \end{Bmatrix} \\
(1 - g^2\nabla^2)\begin{Bmatrix} M_{xx}^{\mathrm{s}} \\ M_{yy}^{\mathrm{s}} \\ M_{xy}^{\mathrm{s}} \end{Bmatrix} &= \left\{\frac{1}{84}\begin{bmatrix} D_{11} & D_{12} & 0 \\ D_{21} & D_{22} & 0 \\ 0 & 0 & D_{66} \end{bmatrix} + \frac{h^2}{12}\begin{bmatrix} (2\mu^s + \lambda^s) & (\tau^s + \lambda^s) & 0 \\ (\tau^s + \lambda^s) & (2\mu^s + \lambda^s) & 0 \\ 0 & 0 & \frac{1}{2}(2\mu^s - \tau^s) \end{bmatrix}\right\}\begin{Bmatrix} \kappa_{xx}^{\mathrm{s}} \\ \kappa_{yy}^{\mathrm{s}} \\ \kappa_{xy}^{\mathrm{s}} \end{Bmatrix} \\
(1 - g^2\nabla^2)\begin{Bmatrix} Q_{yz} \\ Q_{xz} \end{Bmatrix} &= \left\{\begin{bmatrix} A_{44} & 0 \\ 0 & A_{55} \end{bmatrix} + \begin{bmatrix} 2\tau^s & 0 \\ 0 & 2\tau^s \end{bmatrix}\right\}\begin{Bmatrix} \partial w^{\mathrm{s}}/\partial y \\ \partial w^{\mathrm{s}}/\partial x \end{Bmatrix}
\end{aligned} \tag{11}$$

doi: 10.1049/mnl.2014.0651

simply-supported boundary condition, are expressed by

$$W^{\mathrm{b}} = \sum_{m=1}^{\infty}\sum_{n=1}^{\infty} W_{mn}^{\mathrm{b}} \sin(\alpha x)\sin(\beta y)$$
$$W^{\mathrm{s}} = \sum_{m=1}^{\infty}\sum_{n=1}^{\infty} W_{mn}^{\mathrm{s}} \sin(\alpha x)\sin(\beta y) \tag{17}$$

where $\alpha = m\pi/a$ and $\beta = n\pi/b$. m and n are the half-wave number along the x and the y direction. Substituting (17) into (16), the following system of equations are obtained

$$\begin{bmatrix} S_{11} & S_{12} \\ S_{21} & S_{22} \end{bmatrix} \begin{Bmatrix} W_{mn}^{\mathrm{b}} \\ W_{mn}^{\mathrm{s}} \end{Bmatrix} = \begin{Bmatrix} 0 \\ 0 \end{Bmatrix} \tag{18}$$

where

$$\begin{aligned} S_{11} &= \left\{\left(D + \frac{E^{\mathrm{s}}h^2}{2}\right)(\alpha^2+\beta^2)^2\right\} \\ &\quad + \left(2\tau^{\mathrm{s}} + N - \omega^2\frac{\rho h^3}{12}\right)\left\{(\alpha^2+\beta^2) + g^2(\alpha^2+\beta^2)^2\right\} \\ &\quad - \omega^2\rho h\left\{1 + g^2(\alpha^2+\beta^2)\right\} \\ S_{12} &= S_{21} = (2\tau^{\mathrm{s}} + N)\left\{(\alpha^2+\beta^2) + g^2(\alpha^2+\beta^2)^2\right\} \\ &\quad - \omega^2\rho h\left\{1 + g^2(\alpha^2+\beta^2)\right\} \\ S_{22} &= \frac{1}{84}\left\{\left(D + \frac{E^{\mathrm{s}}h^2}{12}\right)(\alpha^2+\beta^2)^2\right\} \\ &\quad + \left(2\tau^{\mathrm{s}} + N - \omega^2\frac{\rho h^3}{12\times 84}\right)\left\{(\alpha^2+\beta^2) + g^2(\alpha^2+\beta^2)^2\right\} \\ &\quad - \omega^2\rho h\left\{1 + g^2(\alpha^2+\beta^2)\right\} \end{aligned} \tag{19}$$

The determinant of the coefficient matrix in (19) must be zero. Therefore the buckling load and fundamental frequency under in-plane biaxial loads are obtained.

3.2. Differential quadrature method: The differential quadrature method reckons partial derivatives of a function at a specific point, as a linear weighted sum of function values at all of the discrete points along the corresponding direction for the variable over the entire domain of that variable. The *mth*-order derivative of a single variable function $f(x)$ at a given grid point i can be approximated by the differential quadrature solution by N grid points as

$$\left.\frac{\partial^m f(x,y)}{\partial x^m}\right|_{(x_i,y_k)} = \sum_{j=1}^{N} C_{ij}^{(m)} f(x_j, y_k), \quad i = 1, 2, \ldots, N \tag{20}$$

where N is the number of grid points in the x-direction and $C_{ij}^{(m)}$ represents the corresponding weight coefficient related to the *mth*-order derivative. For example, if $m = 1$, the first-order derivative is obtained as

$$C_{ij}^{(1)} = \frac{\pi(x_i)}{(x_i - x_j)\pi(x_j)}, \quad i, j = 1, 2, \ldots, N, \quad i \neq j$$
$$C_{ii}^{(1)} = -\sum_{\substack{j=1 \\ j\neq i}}^{N} C_{ij}^{(1)}, \quad i = 1, 2, \ldots, N, \quad i = j \tag{21}$$

where

$$\pi(x_i) = \prod_{j=1}^{N}(x_i - x_j), \quad i, j = 1, 2, \ldots, N, \quad i \neq j \tag{22}$$

The weight coefficients for second- and higher-order derivatives are obtained by using the following simple recursion relationship

$$C_{ij}^{(2)} = \sum_{k=1}^{N} C_{ik}^{(1)} C_{kj}^{(1)}, \quad C_{ij}^{(3)} = \sum_{k=1}^{N} C_{ik}^{(1)} C_{kj}^{(2)}$$
$$C_{ij}^{(4)} = \sum_{k=1}^{N} C_{ik}^{(1)} C_{kj}^{(3)}, \quad i, j = 1, 2, \ldots, N \tag{23}$$

The number of grid points and their distribution can be selected arbitrarily in the implementation of the DQM. Based on the Gauss-Chebyshev-Lobatto grid point distribution [26], the coordinates of the grid points are obtained, as follows

$$x_i = \frac{a}{2}\left(1 - \cos\left(\frac{i-1}{N-1}\pi\right)\right), \quad i = 1, 2, \ldots, N$$
$$y_j = \frac{b}{2}\left(1 - \cos\left(\frac{j-1}{M-1}\pi\right)\right), \quad j = 1, 2, \ldots, M \tag{24}$$

where N and M are the numbers of grid points in the x and y directions, respectively.

4. Results and discussion: The material properties are taken as those of silver nanoplate. The material properties of the nanoplate are: $E = 76$ G*Pa*, $\nu = 0.3$, $\rho = 2250$ kg/m^3, $E^{\mathrm{s}} = 1.22$ N/m and $\tau^{\mathrm{s}} = 0.89$ N/m. Suppose $h = 2$ nm, $\mu^{\mathrm{s}} = 0.47$ N/m and $\lambda^{\mathrm{s}} = 0.28$ N/m.

For buckling analysis, the buckling ratios are defined as (see (25)), where the buckling load is introduced by N_{cr}. For biaxial buckling $N_{xx} = N_{yy} = N_{\mathrm{cr}}$, $N_{xy} = 0$, and for shear buckling $N_{xx} = N_{yy} = 0$, $N_{xy} = N_{cr}$. For vibration analysis, the natural frequency ratios are expressed as (see (26)).

The dimensionless in-plane compressive loadings are introduced by $P = N a^2/D$. The in-plane compressive load for biaxial loading is $N_{xx} = N_{yy} = N$, $N_{xy} = 0$, and and for shear loading is $N_{xx} = N_{yy} = 0$, $N_{xy} = N$. For the sake of brevity, a six-letter symbol is used to represent the boundary conditions for the following four edges of the rectangular nanoplate, as shown in Fig. 2.

$$R_{\mathrm{Snl/nl}} = \frac{\text{buckling load with non-local + surface effects}}{\text{buckling load with non-local effects but without surface effects}}$$
$$R_{\mathrm{Snl/l}} = \frac{\text{buckling load with non-local + surface effects}}{\text{buckling load without both non-local and surface effects}} \tag{25}$$

$$\Omega_{\mathrm{Snl/nl}} = \frac{\text{natural frequency with non-local + surface effects}}{\text{natural frequency with non-local effects but without surface effects}} \tag{26}$$

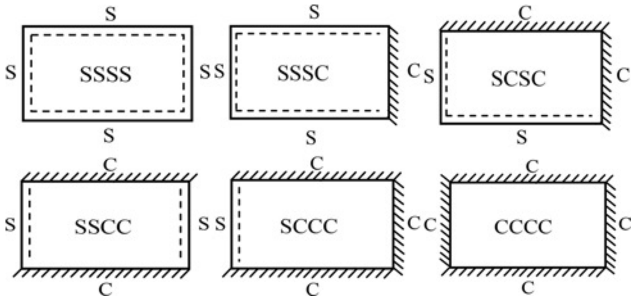

Figure 2 *Combinations of boundary conditions*
S: simply-supported, C: clamped

In the FSDT presented by [22, 23], the non-local effect is considered only for nanoplate bulk, while in the NFSDT presented by Malekzadeh and Shojaee [21], and the presented TVRPT, the local effect is considered for both nanoplate bulk and surface. In addition, in NFSDT, the two theories of FSDT and TVRPT are combined such that the displacement corresponding to shear, u^s, is ignored and instead, the shear correction factor, K_s, is added indirectly. However, in the presented TVRPT, the displacement, u^s, is implemented directly. Consequently, the surface effect for shear is considered in the formulation directly. Tables 1 and 2 indicate the dimensionless biaxial buckling load and natural frequencies of simply-supported square nanoplates considering the surface effects, respectively. From these Tables, it is observed that the presented results are in good agreement with those of others reported in the literature.

From the authors' viewpoint, a $R_{\mathrm{Snl/nl}}$-type parameter for studying the influence of non-localness on the surface effect needs to be defined. Only the surface effect appearing in both the numerator and the denominator of the $R_{\mathrm{Snl/nl}}$-type parameter would be variable, while in the $R_{\mathrm{Snl/l}}$-type parameter, both non-local and surface effects are variables in its numerator and denominator. Thus, increasing the non-local parameter in the $R_{\mathrm{Snl/nl}}$-type parameter, means that the effects of surface parameter need to be observed. In comparison, for the $R_{\mathrm{Snl/l}}$-type parameter, the degree of changes for both parameters would inevitably need to be observed. We should note that

Table 1 Comparison of dimensionless biaxial buckling load ($N_{cr}a^2/D$) for square nanoplates with all edges simply-supported ($a = 10$ nm)

g^2, (nm^2)	References		$a/h = 2$	5	10
0	[22]	FSDT	8.4543	19.8741	45.8043
	[21]	NFSDT	8.5249	19.9869	45.8842
	present	TVRPT	8.6052	19.9950	45.8849
1	[22]	FSDT	7.1039	17.2182	42.7225
	[21]	NFSDT	7.1533	17.2191	42.5363
	present	TVRPT	7.2204	17.2258	42.5369

Table 2 Comparison of dimensionless natural frequencies ($\omega a^2(\rho h/D_{11})^{0.5}$) for square nanoplates with all edges simply-supported ($a = 10$ nm, $P = 0$)

g^2, $(nm)^2$	References		$a/h = 2$	5	10
0	[23]	FSDT	12.4500	19.3883	29.8513
	[21]	NFSDT	12.4942	19.4378	29.8757
	present	TVRPT	12.5359	19.4412	29.8759
1	[23]	FSDT	11.4139	18.0474	28.8200
	[21]	NFSDT	11.4448	18.0417	28.7651
	present	TVRPT	11.4828	18.0446	28.7652

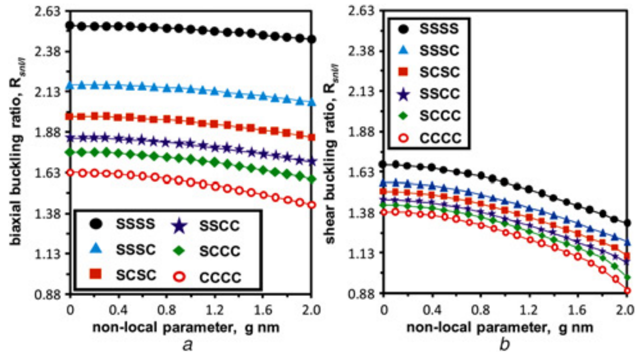

Figure 3 *Buckling ratio, $R_{Snl/l}$, against non-local parameter for various boundary conditions, ($a = b = 30$ nm)*
a Biaxial buckling
b Shear buckling

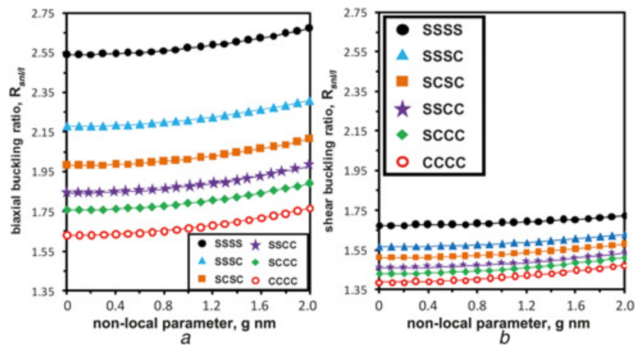

Figure 4 *Buckling ratio, $R_{Snl/nl}$, against non-local parameter for various boundary conditions, ($a = b = 30$ nm)*
a Biaxial buckling
b Shear buckling

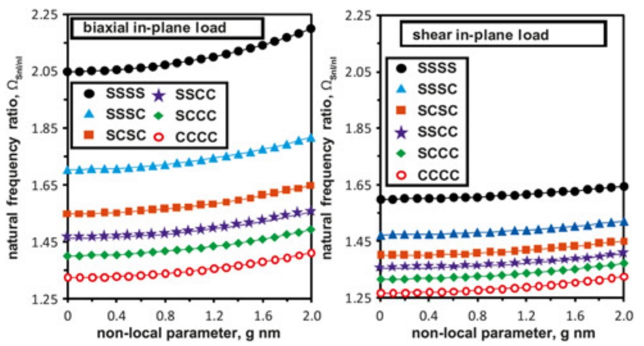

Figure 5 *Natural frequency ratio, $\Omega_{Snl/nl}$, against non-local parameter for various boundary conditions, ($a = b = 30$ nm, $P = 10$)*
a Biaxial in-plane load
b Shear in-plane load

some authors [21–23] used the $R_{\mathrm{Snl/l}}$-type parameter and mentioned that by augmenting the non-local parameter, the surface effects on both buckling and vibration would diminish.

Figs. 3–5, respectively, show the effects of the non-local parameter on the $R_{\mathrm{Snl/l}}$, $R_{\mathrm{Snl/nl}}$ and $\Omega_{\mathrm{Snl/nl}}$-type parameters of a square nanoplate for the above-mentioned boundary conditions. From Fig. 3, it can be seen that by augmenting the non-local parameter, the $R_{\mathrm{Snl/l}}$-type parameter reduces. Moreover, it is observed that the non-local effects are more pronounced for the CCCC boundary condition, as compared with the SSSS boundary condition. Therefore the effect of the non-local parameter seems to show itself in the following order of magnitude for different in-plane loading and different boundary conditions

Micro & Nano Letters, 2015, Vol. 10, Iss. 6, pp. 276–281
doi: 10.1049/mnl.2014.0651

in buckling problems, respectively: biaxial and shear, and SSSS, SSSC, SCSC, SSCC, SCCC and CCCC. For biaxial buckling problems, the in-plane compressive loading is applied from all four sides of the plate, while for shear buckling problems, this in-plane shear loading could be equivalent to two uniaxial compressive and tensile crossing loads on the principal planes and directions. Thus, the plate stiffness should be the highest for the shear buckling case, and the lowest for the biaxial case.

From Figs. 4 and 5, it is found that as the boundary conditions become more rigid, the $R_{\rm Snl/nl}$ and $\Omega_{\rm Snl/nl}$-type parameters decrease. Therefore the surface effects would reduce. In addition, as the value of the non-local parameter rises, the $R_{\rm Snl/nl}$ and $\Omega_{\rm Snl/nl}$-type parameters would advance; therefore the surface effects would also rise. Therefore the degree of surface effect seems to exhibit itself in the following order of magnitude for different in-plane loading and different boundary conditions, respectively: shear and biaxial, and CCCC, SCCC, SSCC, SCSC, SSSC and SSSS. The non-local parameter would seem to have a compliant effect on the structural behaviour of a plate, while the surface effect parameter would have a stiffening effect. Having this in mind, by increasing the non-local parameter, both the numerator and denominator of the $R_{\rm Snl/nl}$ and $\Omega_{\rm Snl/nl}$-type parameters would decrease simultaneously, but because of the presence of the surface effect parameter in the numerator, it would be decreased less than its denominator. Thus, the $R_{\rm Snl/nl}$ and $\Omega_{\rm Snl/nl}$-type parameters would be raised. Consequently, by augmenting the non-local parameter further, these $R_{\rm Snl/nl}$ and $\Omega_{\rm Snl/nl}$-type parameters would get larger and the surface effect would show itself more. As far as switching from the boundary conditions having the property of completely free rotations, such as simply-support, towards the boundary conditions having more restraint on the rotations, for example, clamped, as well as switching from biaxial loading towards shear loading, the non-local effect would indicate itself more strongly since this effect could have an inherent compliant property. It is noted that biaxial loading is classified as the worst loading, but shear loading as the most stable loading, because of producing more stiffness in the plate during buckling and vibration. On the contrary, the surface effect would manifest itself weaker, since it could have an inherent property of stiffening.

5. Conclusions: In this Letter, surface effects and non-local two variable refined plate theories are combined and investigated on the shear/biaxial buckling and vibration of a rectangular nanoplate. The differential quadrature method was applied to solve the governing equations for buckling and vibrations of a nanoplate. The non-local effects on the surface effects of shear/biaxial buckling and vibration were investigated for various boundary conditions. It was found that non-local parameters were significant regarding the surface effects. In addition, the surface effects on the buckling and vibration were remarkable such that they cannot be ignored. From the results of the present study, the following conclusions are important:

- As the boundary conditions become stiffer, that is, moving from SSSS towards CCCC, the non-local effects would increase, but the surface effects on the buckling and vibration reduced.

- The effects of the non-local parameter on the shear buckling and vibration were more notable than that of the biaxial, while the values of surface effects on the biaxial buckling and vibration were more important than that of shear.

- By increasing the non-local parameter, the values of surface effects on the buckling and vibration were enhanced. This result was in contrast to the works of other researchers in the field.

6 References

[1] Lim C.W., He L.H.: 'Size-dependent nonlinear response of thin elastic films with nanoscale thickness', *Int. J. Mech. Sci.*, 2004, **46**, pp. 1715–1726

[2] Huang D.W.: 'Size-dependent response of ultra-thin films with surface effects', *Int. J. Solids. Struct.*, 2008, **45**, pp. 568–579

[3] Assadi A., Farshi B., Ali A.-Z.: 'Size dependent dynamic analysis of nanoplates', *J. Appl. Phys.*, 2010, **107**, p. 124310

[4] Assadi A.: 'Size dependent forced vibration of nanoplates with consideration of surface effects', *Appl. Math. Model*, 2013, **37**, pp. 3575–3588

[5] Assadi A., Farshi B.: 'Vibration characteristics of circular nanoplates', *J. Appl. Phys.*, 2010, **108**, p. 74312

[6] Assadi A., Farshi B.: 'Size dependent stability analysis of circular ultrathin films in elastic medium with consideration of surface energies', *Physica E*, 2011, **43**, pp. 1111–1117

[7] Ansari R., Shahabodini A., Shojaei M.F., Mohammadi V., Gholami R.: 'On the bending and buckling behaviors of Mindlin nanoplates considering surface energies', *Physica E*, 2014, **57**, pp. 126–137

[8] Wang K.F., Wang B.L.: 'A finite element model for the bending and vibration of nanoscale plates with surface effect', *Finite. Elem. Anal. Des.*, 2013, **74**, pp. 22–29

[9] Malekzadeh P., Haghighi M.R.G., Shojaee M.: 'Nonlinear free vibration of skew nanoplates with surface and small scale effects', *Thin. Wall. Struct.*, 2014, **78**, pp. 48–56

[10] Farajpour A., Dehghany M., Shahidi A.R.: 'Surface and nonlocal effects on the axisymmetric buckling of circular graphene sheets in thermal environment', *Compos. B*, 2013, **50**, pp. 333–343

[11] Asemi S.R., Farajpour A.: 'Decoupling the nonlocal elasticity equations for thermo-mechanical vibration of circular graphene sheets including surface effects', *Physica E*, 2014, **60**, pp. 80–90

[12] Mahmoud F.F., Eltaher M.A., Alshorbagy A.E., Meletis E.I.: 'Static analysis of nanobeams including surface effects by non-local finite element', *J. Mech. Sci. Tech.*, 2012, **26**, pp. 3555–3563

[13] Eltaher M.A., Mahmoud F.F., Assie A.E., Meletis E.I.: 'Coupling effects of nonlocal and surface energy on vibration analysis of nanobeams', *Appl. Math. Comput.*, 2013, **224**, pp. 760–774

[14] Mohammadi M., Goodarzi M., Ghayour M., Alivand S.: 'Small scale effect on the vibration of orthotropic plates embedded in an elastic medium and under biaxial in-plane pre-load via nonlocal elasticity theory', *J. Solid. Mech.*, 2012, **4**, pp. 128–143

[15] Mohammadi M., Farajpour A., Goodarzi M., Shehni nezhad pour H.: 'Numerical study of the effect of shear in-plane load on the vibration analysis of graphene sheet embedded in an elastic medium', *Comput. Mater. Sci.*, 2014, **82**, pp. 510–520

[16] Mohammadi M., Farajpour A., Moradi A., Ghayour M.: 'Shear buckling of orthotropic rectangular graphene sheet embedded in an elastic medium in thermal environment', *Compos. B*, 2014, **56**, pp. 629–637

[17] Shimpi R.P.: 'Refined plate theory and its variants', *AIAA J.*, 2002, **40**, pp. 137–146

[18] Narendar S., Gopalakrishnan S.: 'Scale effects on buckling analysis of orthotropic nanoplates based on nonlocal two-variable refined plate theory', *Acta. Mech.*, 2012, **223**, pp. 395–413

[19] Narendar S.: 'Buckling analysis of micro-/nano-scale plates based on two-variable refined plate theory incorporating nonlocal scale effects', *Compos. Struct.*, 2011, **93**, pp. 3093–3103

[20] Malekzadeh P., Shojaee M.: 'Free vibration of nanoplates based on a nonlocal two-variable refined plate theory', *Compos. Struct.*, 2013, **95**, pp. 443–452

[21] Malekzadeh P., Shojaee M.: 'A two-variable first-order shear deformation theory coupled with surface and nonlocal effects for free vibration of nanoplates', *J. Vib. Control.*, 2013, doi: 10.1177/1077546313516667

[22] Wang K.F., Wang B.L.: 'Combining effects of surface energy and non-local elasticity on the buckling of nanoplates', *Micro Nano Lett.*, 2011, **6**, pp. 941–943

[23] Wang K.F., Wang B.L.: 'Vibration of nanoscale plates with surface energy via nonlocal elasticity', *Physica E.*, 2011, **44**, pp. 448–453

[24] Eringen A.C., Edelen D.G.B.: 'On nonlocal elasticity', *Int. J. Eng. Sci.*, 1972, **10**, pp. 233–248

[25] Gurtin M.E., Murdoch A.I.: 'Surface stress in solids', *Int. J. Solids. Struct.*, 1978, **14**, pp. 431–440

[26] Shu C.: 'Differential quadrature and its application in engineering' (Springer, Berlin, 2000)